LETTERS

Low Atlantic hurricane activity in the 1970s and 1980s compared to the past 270 years

Johan Nyberg[1], Björn A. Malmgren[2], Amos Winter[3], Mark R. Jury[4], K. Halimeda Kilbourne[5,6] & Terrence M. Quinn[5,7,8]

Hurricane activity in the North Atlantic Ocean has increased significantly since 1995 (refs 1, 2). This trend has been attributed to both anthropogenically induced climate change[3] and natural variability[1], but the primary cause remains uncertain. Changes in the frequency and intensity of hurricanes in the past can provide insights into the factors that influence hurricane activity, but reliable observations of hurricane activity in the North Atlantic only cover the past few decades[2]. Here we construct a record of the frequency of major Atlantic hurricanes over the past 270 years using proxy records of vertical wind shear and sea surface temperature (the main controls on the formation of major hurricanes in this region[1,3–5]) from corals and a marine sediment core. The record indicates that the average frequency of major hurricanes decreased gradually from the 1760s until the early 1990s, reaching anomalously low values during the 1970s and 1980s. Furthermore, the phase of enhanced hurricane activity since 1995 is not unusual compared to other periods of high hurricane activity in the record and thus appears to represent a recovery to normal hurricane activity, rather than a direct response to increasing sea surface temperature. Comparison of the record with a reconstruction of vertical wind shear indicates that variability in this parameter primarily controlled the frequency of major hurricanes in the Atlantic over the past 270 years, suggesting that changes in the magnitude of vertical wind shear will have a significant influence on future hurricane activity.

The years from 1995 to 2005 experienced an average of 4.1 major Atlantic hurricanes (category 3 to 5) per year, while the years 1971 to 1994 experienced an average of 1.5 major hurricanes per year[2]. A major hurricane is defined as a tropical cyclone with maximum sustained (1 minute) surface (measured 10 m above the surface) winds of $\geq 50\ m\ s^{-1}$. This increase in major hurricane frequency is thought to be caused by weaker vertical wind shear $|V_z|$ and warmer sea surface temperatures (SSTs) in the tropical and subtropical Atlantic[1,3], which some studies have attributed to a natural multidecadal variability in the thermohaline circulation[1], termed the Atlantic Multidecadal Oscillation (AMO)[6], and other studies to anthropogenic climate change[3]. Little information exists about the effects of the AMO variability on changes in tropical Atlantic climate and magnitudes of hurricane activity. Although hurricane intensity and destructiveness may increase with increasing global mean temperatures[3,7], the effect of climate warming on hurricane frequency is poorly known[8]. Furthermore, it is possible that hurricane activity responds to changes in other external forcings, such as solar activity[9] and aerosol loading[3]. The reliable observation record of hurricane activity over the North Atlantic exists only from 1944 (ref. 2) with continual satellite coverage from 1966 (ref. 10), providing a temporally limited perspective on these issues. The existing historical records of hurricane activity are based on archives documenting primarily US landfalls[11].

The Main Development Region (MDR)[1,5] is where 85% of all Atlantic major hurricanes and 60% of all non-major hurricanes (33 to 50 $m\ s^{-1}$) and tropical storms (18 to 32 $m\ s^{-1}$) are formed. The MDR is an area westward of Africa across the tropical Atlantic and Caribbean Sea at latitudes between 10° and 20° N (Figs 1 and 2). Here tropical cyclones are formed when easterly atmospheric waves propagate from Africa across the tropical North Atlantic[1,5]. Because the number of easterly waves are fairly constant from year to year[1,12], the dominant factors for major hurricane formation are the magnitude of $|V_z|$, and SSTs in the MDR during August to October, when almost all major hurricanes are formed[1,3–5,13]. Local vertical wind shear $|V_z| > \sim 8\ m\ s^{-1}$ (for example, upper winds opposed to lower easterly trade winds) is in general unfavourable for the formation of tropical cyclones owing to distortion of the vertical structure of the convective cloud cells[14]. The vertically tilted cloud cells are limited in their capacity to provide energy to the storm.

Local SSTs of ~27 °C or more and a warm mixed layer down to a depth of ~50 m are also considered necessary for major hurricane development[1,4]. Empirical studies indicate, however, that warmer local SSTs are not central in the formation of major hurricanes[1,4]. Regional Atlantic SSTs appear to be more important for the formation of major hurricanes through their interdependence with $|V_z|$ in the MDR[1,4], which may arise from interactions with the Pacific El Niño Southern Oscillation (ENSO)[15]. Warmer SSTs in the North Atlantic region coincide with reduced $|V_z|$ in the MDR and vice versa[1,4].

Comparisons between the hurricane index[2] and observed zonal winds show significant positive (westerly) correlation values from the surface up to 1.5 km (850 hPa) over latitudes ~10–20° N (Fig. 1), while significant negative (easterly) correlation values exist around 12 km (200 hPa) in these latitudes. Consequently, by using proxies of $|V_z|$ (trade wind strength) and SST anomalies in the MDR, robust longer-term estimations of major hurricane activity are possible.

To estimate $|V_z|$ we use four luminescence intensity records for the months August to October derived from coral cores[16] retrieved in the Caribbean off the southern Dominican Republic, south-western Puerto Rico and Mona Island together with one annual abundance record of the planktonic foraminifer *Globigerina bulloides* in a well-dated (^{14}C and ^{210}Pb) sediment core[17] from the Cariaco basin in the southern Caribbean Sea (Fig. 2a–d).

The significant relationships shown in Fig. 2a–d (see also Supplementary Information) are explained as follows: luminescence intensity in corals reflects the degree of terrestrial runoff, which is controlled by the amount of precipitation[16]. Decreased precipitation

[1]Geological Survey of Sweden, Box 670, SE-751 28 Uppsala, Sweden. [2]Department of Earth Sciences, Göteborg University, Box 460, SE-405 30 Göteborg, Sweden. [3]Department of Marine Sciences, University of Puerto Rico, PO Box 9013. [4]Department of Physics, University of Puerto Rico, PO Box 9016, PR 00681-9013, Mayagüez, Puerto Rico. [5]College of Marine Science, University of South Florida, 140, St Petersburg, Florida 33707, USA. [6]Physical Sicences Division R/PSD1, NOAA, Earth System Research Laboratory, 325 Broadway, Boulder, Colorado 80305, USA. [7]Department of Geological Sciences, Jackson School of Geosciences, University of Texas at Austin, 1 University Station C1100, Austin, Texas 78712, USA. [8]Institute for Geophysics, J. J. Pickle Research Campus, University of Texas at Austin, 10100 Burnet Road, Austin, Texas 78758, USA.

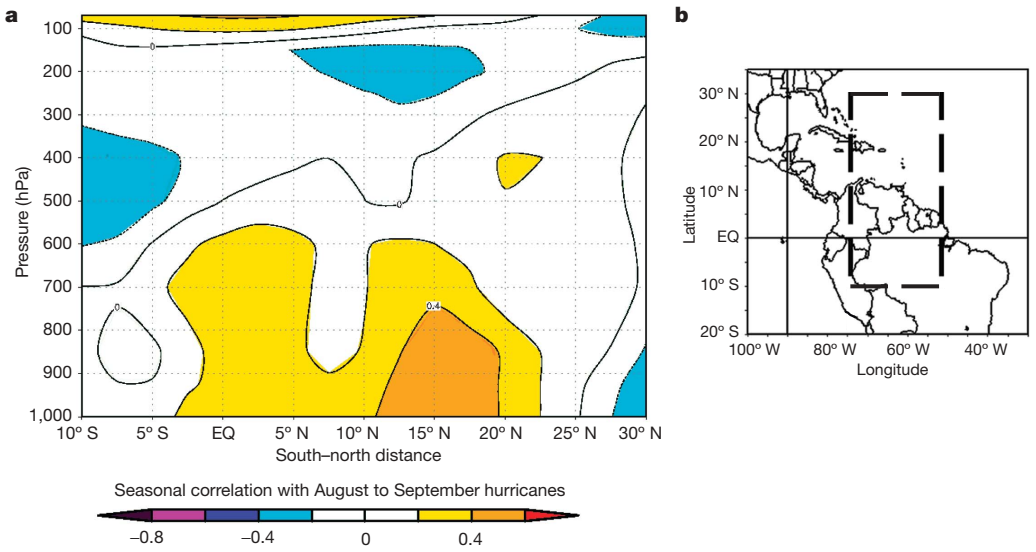

Figure 1 | Simultaneous correlation of zonal winds in August-September (1955–2004) with the unsmoothed Atlantic hurricane index[2]. NCEP/NCAR Reanalysis (285° E to 310° E). Positive (or negative) values on the colour scale refer to increased westerlies (or easterlies) in active hurricane years. Correlation values exceeding ±0.2 are significant above the 90% confidence level. The zonal winds are within the area marked by dashed lines in **b**.

in the northeastern Caribbean during the hurricane season is associated with increased trade-wind speed and high $|V_z|$ over the MDR[16,18,19] (Fig. 2). Increased trade-wind speed corresponds to higher sea-level pressures, enhanced sinking motion and drying and a more stable lower atmosphere, which results in lower precipitation and a more sheared environment in the tropical Atlantic during the hurricane season[18]. Higher abundance of *G. bulloides* reflects more nutrient supply caused by enhanced upwelling due to increased trade-wind strength, which is related to high $|V_z|$ over the MDR[17] (Fig. 2d, see also Supplementary Information). In addition, these wind-speed records are tightly linked to larger-scale SST anomalies in the North Atlantic region[16,17], which supports their robustness as a proxy of major hurricane activity. Figure 2a–d also displays an association between these four proxies and $|V_z|$ north of the MDR that is out of phase with $|V_z|$ within the MDR, supporting instrumental observations of an out-of-phase relationship between horizontal wind shear on either side of the main track of Atlantic hurricanes[5].

Back propagation artificial neural networks were used to estimate past $|V_z|$ and major hurricane activity. The networks were trained to

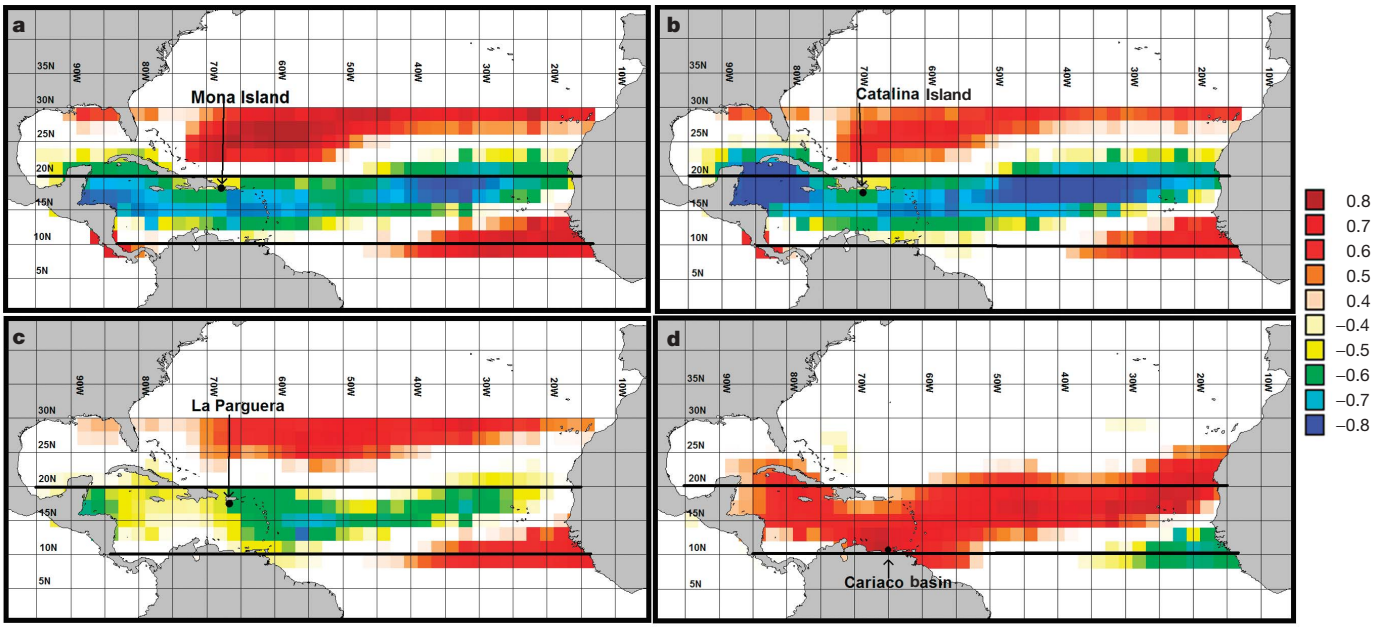

Figure 2 | Spatial correlations between instrumentally observed vertical windshear ($|V_z|$) in August–October and the proxies used. Luminescence intensity during August to October in the coral cores retrieved outside Mona Island, 1949–1992 (**a**), Catalina Island, 1949–1993 (**b**) and La Parguera, 1949–2000 (**c**). **d**, Annual abundance of the planktonic foraminifer *Globigerina bulloides* in the Cariaco basin, 1949–1990. The colour scale refers to all panels. Only statistically significant correlation values exceeding the 0.01 ($r_S < -0.4$ and $r_S > 0.4$) and 0.001 ($r_S < -0.5$ and $r_S > 0.5$) levels are shown and referred to in the colour scale. Solid lines in **a**–**d** give the north and south boundaries of the MDR.

learn the relationships between the combined input (independent) proxy records and each of the two output (dependent) instrumental records of $|V_z|$ and number of major hurricanes, respectively (Fig. 3). The SST anomaly record[20] was averaged between latitudes of 10 and 25° N and longitudes of 20 to 85° W, because the region where SST anomalies directly affect major hurricane activity is within and around the MDR[4,21]. Although instrumentally recorded $|V_z|$, luminescence intensity and *G. bulloides* show the strongest correlations with SST anomalies in the North Atlantic region between 50 and 60° N (refs 1, 16 and 17), these records also show statistical significant relationships with the instrumental SST anomaly record[20,22], averaged over the MDR, using five-year running averages (Fig. 3). This demonstrates the physical link between SST anomalies in the MDR and $|V_z|$.

Figure 3 shows that the switch from low to high abundance of *G. bulloides*, high to low luminescence intensity, and high to low SST anomalies is coincident with the shift towards high-$|V_z|$ conditions and decreased major hurricane activity in the period 1965–1971 (refs 1, 2). The shift back towards low $|V_z|$ conditions and increased major hurricane activity starts around 1987–1988, but is suppressed by the long-lasting (1990–1995) El Niño event[1] (Fig. 3). The record of *G. bulloides* (until 1990) reflects the shift around 1987–1988, while the luminescence-intensity records reflect both the El Niño event (1990–1995) and the evident shift towards increased major hurricane activity around 1995 (ref. 1 and Fig. 3).

The downward trend in the frequency of major hurricanes[23] from the 1940s to 1970s in the reliable observation record is matched by the

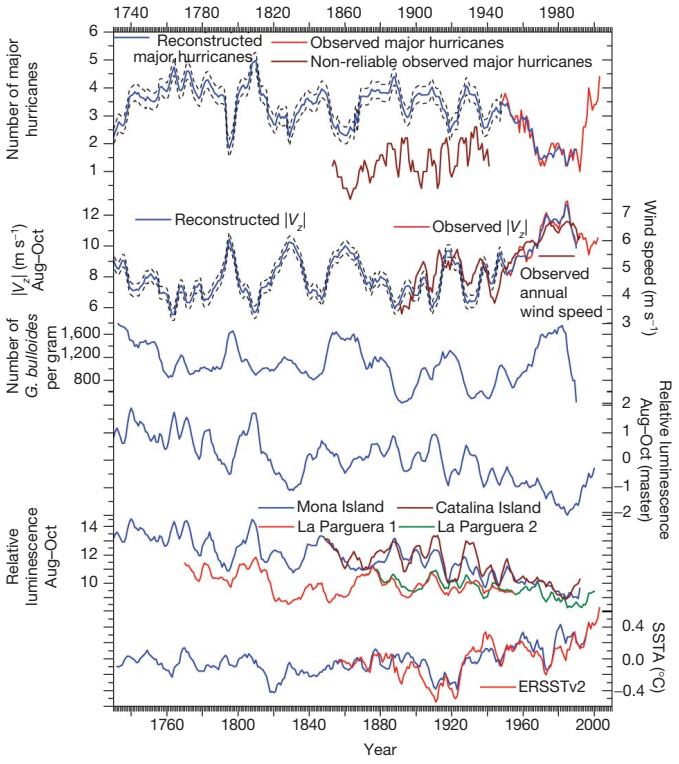

Figure 3 | The reconstructed major hurricane activity and $|V_z|$ series back to 1730. Also shown are the reliable observation records back to 1944 (ref. 2) and 1949 (ref. 19), respectively, the historical hurricane record back to 1851 (refs 10, 11), the ERSST v2 data[22] averaged over 10 to 26° N and 20 to 86° W during August–October back to 1854, zonal wind speed data centred at 11° N and 65° W (ref. 30) back to 1890 together with the SST anomalies[20], luminescence intensities, and abundance of *G. bulloides* upon which the reconstructions were based. The dashed lines indicate 95% confidence intervals for estimated numbers of hurricanes and $|V_z|$ values. All data are smoothed with a five-year running average. The 'master' luminescence curve is developed by averaging standardised luminescence intensity values during Aug–Oct in all of the coral cores for each year.

reconstruction (Fig. 3). The reconstruction also follows the variability during the 19th and 20th centuries of US East Coast hurricane landfalls[2,9,10,23,24], with a quiet period during the 1850s to the late 1860s, an active period from the 1870s to the 1890s, a quiescent period to 1926, and an active phase from 1926 to 1970. We note the reconstructed high activity around 1886, which is the most active hurricane season on record for the continental United States[11]. In addition, the reconstructed $|V_z|$ closely follows observed annual zonal wind speed data in the Caribbean back to 1890, and high reconstructed $|V_z|$ values back to 1851 coincide with low observed major hurricane activity[11] (Fig. 3). The exact numbers of observed major Atlantic hurricanes before 1944 are less accurate owing to the lack of observational networks[2,11], which probably explains the difference between the numbers of reconstructed and instrumentally observed major hurricanes (Fig. 3).

The reconstruction shows that there have been on average ~3–3.5 major hurricanes and a $|V_z|$ of ~8–9 m s^{-1} per year from 1730 to 2005. A gradual downward trend is evident from an average of ~4.1 (1755–1785) to ~1.5 major hurricanes during the late 1960s to early 1990s, which experienced strong $|V_z|$ and few major hurricanes compared to other periods since 1730. Only the periods ~1730–1736, 1793–1799, 1827–1830, 1852–1866 and 1915–1926 appear to have been marked by similarly low major hurricane activity and high $|V_z|$. Furthermore, the current active phase (1995–2005) is unexceptional compared to the other high-activity periods of ~1756–1774, 1780–1785, 1801–1812, 1840–1850, 1873–1890 and 1928–1933 (Fig. 3), and appears to represent a recovery to normal hurricane activity, despite the increase in SST.

Wavelet spectral analyses together with spectral analyses reveal the existence of significant ~8–11 and ~20–30-year cycles in the records (see Supplementary Information). Decadal signals in occurrences, formation areas, and landfalls of tropical storms and hurricanes have also been identified elsewhere and linked to the North Atlantic Oscillation[9,24,25].

To improve our understanding further, the derived records are compared with indices of the AMO[6,26] and total solar irradiance (TSI)[27] (Fig. 4). Reduced major hurricane activity coincides with a lower AMO index around 1820–1830, 1910–1920 and 1970–1990; enhanced activity coincides with a high index around 1750–1790, 1870–1900 and 1930–1960 (Fig. 4). Peaks and trends of higher major hurricane activity concur with lower TSI, and vice versa, several times since 1730 (Fig. 4). Results from a general circulation model show that circulation changes in the upper stratosphere, induced by interactions between solar irradiance and ozone levels, may penetrate

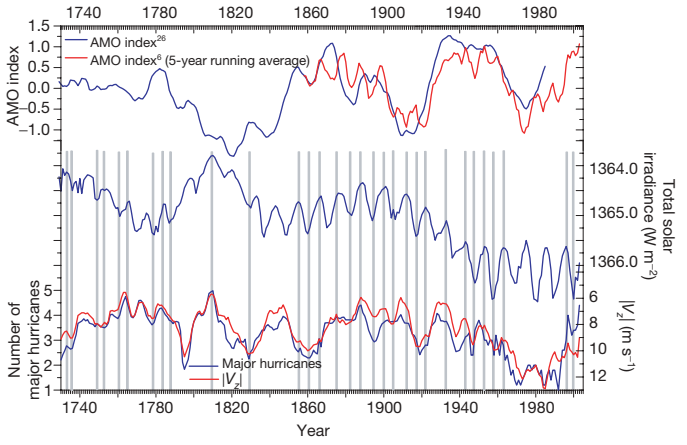

Figure 4 | The reconstructed major hurricane and $|V_z|$-series compared to total solar irradiance and AMO indices. The instrumental records of major hurricane activity and $|V_z|$ (five-year running averages) are shown from 1944 and 1949, respectively, to 2005. TSI and $|V_z|$ have increasing values downwards. Shaded lines mark concurrent peaks and lows in TSI, hurricane activity and/or $|V_z|$.

down to the troposphere, where surface winds and sea level pressures are affected[28]. In addition, the general circulation model shows a forced shift towards decreased sea level pressure in the subtropical Atlantic during reduced TSI, which would result in weaker easterly trade winds, weaker $|V_z|$ and higher major hurricane activity, and thus explains some of our observations.

Our results suggest that the frequency of major hurricanes since 1995 is not unusual, indicating that increases in SST during the past 270 years have been offset by increased $|V_z|$, which suppresses major hurricanes. A more rapid warming of the atmosphere relative to the ocean could have caused the anomalous calm period between the 1970s and 1990s. Air temperatures near the level of the trade-wind inversion (1.5 km) as well as 10 m air temperatures during the past 50 and 100 years, respectively, averaged over the Caribbean (see Supplementary Information), have risen faster than SSTs, indicating an enhanced stability of the lower atmosphere and a strengthening of the trade-wind inversion that reduces the influence of thermodynamic energy from a warmer ocean[29]. This physical mechanism leads to enhanced subsidence, trade-wind strength and $|V_z|$ in the MDR[29]. The reconstructed $|V_z|$ series may indicate that this trend has occurred over a longer period.

The future possibility of lower $|V_z|$ combined with increased SSTs in the MDR (Figs 3 and 4) may result in longer storm lifetimes and more moist enthalpy to power developing tropical cyclones, causing higher hurricane frequencies and greater storm intensities.

METHODS SUMMARY

The correlation coefficients are computed using the Spearman rank correlation (r_S) owing to the presumed lack of non-normality of the data series. The statistical significances are judged using a two-tailed significance test. The vertical wind shear V_z is calculated as the vector difference between the 200 and 850 mbar climatological winds[1] averaged for August–October from the NCEP/NCAR Reanalysis gridded ($2.5^\circ \times 2.5^\circ$ interval) monthly mean wind data set over the MDR region[19]. A single 'master' coral luminescence intensity curve was developed by averaging standardized luminescence intensity values in all of the four cores for each year.

The Trajan 6.0 Neural Network software was used for the autonomous learning of the relationships between the independent variables (master luminescence intensity, number of *G. bulloides* and SSTs) and dependent variables (number of instrumentally observed major hurricanes and vertical windshear). The data sets were split so that ~67% of the samples was used in the training set, ~20% in the selection set, and the remaining samples in the test set. Each of the reconstructed time series was derived from ensembles constituting ten independent networks. The prediction errors—the root-mean-square errors of predictions—were computed for each network as the square root of the sum of the squared differences between the observed and predicted values divided by the number of samples in the test sets using different training, selection and test cases. The 95% confidence intervals for the estimated values were then based on these ten different runs.

$|V_z|$ and major hurricane activity are associated primarily with the large-scale decadal SST fluctuations in the Atlantic[1,3]. Therefore, to emphasize lower-frequency variations, a five-year running average was used when training the networks. Significance tests account for the additional auto-correlation imposed by the filter.

Full Methods and any associated references are available in the online version of the paper at www.nature.com/nature.

Received 24 October 2006; accepted 1 May 2007.

1. Goldenberg, S. B., Landsea, C. W., Mestas-Nuñez, A. M. & Gray, W. M. The recent increase in Atlantic hurricane activity: causes and implications. *Science* **293,** 474–479 (2001).
2. Jarvinen, B. R., Neumann, C. J. & Davis, M. A. S. A tropical cyclone data tape for the North Atlantic basin, 1886–1983: Contents, limitations, and uses. *NOAA Tech. Memo. NWS NHC* Vol. 22, 1–21 (NOAA, Coral Gables, Florida, 1984).
3. Mann, M. E. & Emanuel, K. A. Atlantic hurricane trends linked to climate change. *Eos* **87,** 233–241 (2006).
4. Shapiro, L. J. & Goldenberg, S. B. Atlantic sea surface temperature and tropical cyclone formation. *J. Clim.* **11,** 578–590 (1998).
5. Goldenberg, S. B. & Shapiro, L. J. Physical mechanisms for the association of El Niño and West African rainfall with Atlantic major hurricane activity. *J. Clim.* **9,** 1169–1187 (1996).
6. Enfield, D. B., Mestas-Nuñez, A. M. & Trimble, P. J. The Atlantic multidecadal oscillation and its relation to rainfall and river flows in the continental U.S. *Geophys. Res. Lett.* **28,** 2077–2080 (2001).
7. Emanuel, K. Increasing destructiveness of tropical cyclones over the past 30 years. *Nature* **436,** 686–688 (2005).
8. Curry, J. A., Webster, P. J. & Holland, G. J. Mixing politics and science in testing the hypothesis that greenhouse warming is causing a global increase in hurricane intensity. *Bull. Am. Meteorol. Soc.* **87,** 1025–1038 (2006).
9. Elsner, J. B., Kara, A. B. & Owens, M. A. Fluctuations in North Atlantic hurricane frequency. *J. Clim.* **12,** 427–437 (1999).
10. Neumann, C. J., Jarvinen, B. R., McAdie, C. J. & Elms, J. D. *Tropical Cyclones of the North Atlantic Ocean, 1871–1998* 11–15 (National Climatic Data Center, Asheville, North Carolina, 1999).
11. Landsea, C. W. *et al.* in *Hurricanes and Typhoons: Past, Present and Future* (Murname, R. J. & Liu, K.-B.) 177–221 (Columbia Univ. Press, New York, 2004).
12. Avila, L. A., Pasch, R. J. & Jiing, J.-G. Atlantic tropical systems of 1996 and 1997: years of contrasts. *Mon. Weath. Rev.* **128,** 3695–3706 (2000).
13. Aiyyer, A. R. & Thorncroft, T. Climatology of vertical wind shear in the tropical Atlantic. *J. Clim.* **19,** 2969–2983 (2006).
14. DeMaria, M., Balk, J.-J. & Kaplan, J. Upper-level eddy angular momentum fluxes and tropical cyclone intensity change. *J. Atmos. Sci.* **50,** 1133–1147 (1993).
15. Dong, B., Sutton, R. T. & Scaife, A. A. Multidecadal modulation of El Niño–Southern Oscillation (ENSO) variance by Atlantic Ocean sea surface temperatures. *Geophys. Res. Lett.* **33,** L08705, doi:10.1029/2006GL025766 (2006).
16. Nyberg, J. Luminescence intensity in coral skeletons from Mona Island in the Caribbean Sea and its link to precipitation and wind speed. *Phil. Trans. R. Soc. Lond. A* **360,** 749–766 (2002).
17. Black, D. E. *et al.* Eight centuries of North Atlantic ocean atmosphere variability. *Science* **286,** 1709–1713 (1999).
18. Knaff, J. A. Implications of summertime sea level pressure anomalies in the tropical Atlantic region. *J. Clim.* **10,** 789–804 (1997).
19. Kalnay, E. *et al.* The NCEP/NCAR 40-year reanalysis. *Bull. Am. Meteorol. Soc.* **77,** 437–471 (1996).
20. Mann, M. E., Bradley, R. S. & Hughes, M. K. Global-scale temperature patterns and climate forcing over the past six centuries. *Nature* **392,** 779–787 (1998).
21. Vitart, F. & Anderson, J. L. Sensitivity of Atlantic tropical storm frequency to ENSO and interdecadal variability of SSTs in an ensemble of AGCM integrations. *J. Clim.* **14,** 533–545 (2001).
22. Smith, T. M. & Reynolds, R. W. Improved extended reconstruction of SST (1854–1997). *J. Clim.* **17,** 2466–2477 (2004).
23. Landsea, C. W., Nicholls, N., Gray, W. M. & Avila, L. A. Downward trends in the frequency of intense Atlantic hurricanes during the past five decades. *Geophys. Res. Lett.* **23,** 1697–1700 (1996).
24. Elsner, J. B., Jagger, T. & Kocher, B. Changes in the rates of North Atlantic major hurricane activity during the 20th century. *Geophys. Res. Lett.* **27,** 1743–1750 (2000).
25. Elsner, J. B. & Jagger, T. H. Prediction models for annual US hurricane counts. *J. Clim.* **19,** 2935–2952 (2006).
26. Gray, S. T., Graumlich, L. J., Betancourt, J. L. & Pederson, G. T. A tree-ring based reconstruction of the Atlantic Multidecadal Oscillation since 1567 AD. *Geophys. Res. Lett.* **31,** L12205, doi:10.1029/2004GL019932 (2004).
27. Lean, J. 2000. Evolution of the Sun's spectral irradiance since the Maunder Minimum. *Geophys. Res. Lett.* **27,** 2425–2428 (2000).
28. Shindell, D. T. *et al.* Solar forcing of regional climate during the Maunder Minimum. *Science* **294,** 2149–2152 (2001).
29. Held, I. M. & Soden, B. J. Robust responses of the hydrological cycle to global warming. *J. Clim.* **19,** 5686–5699 (2006).
30. Woodruff, S. D., Slutz, R. J., Jenne, R. L. & Steurer, P. M. A comprehensive ocean-atmosphere data set. *Bull. Am. Meteorol. Soc.* **68,** 1239–1250 (1987).

Supplementary Information is linked to the online version of the paper at www.nature.com/nature.

Acknowledgements This work is supported by grants from the Swedish Research Council (to J.N.).

Author Contributions J.N. derived the coral records, the vertical wind shear and hurricane reconstructions and wrote the paper, except for the Fig. 1 legend and parts of the penultimate paragraph, which were written by M.R.J. M.R.J., B.A.M., A.W. and K.H.K. assisted and commented on the manuscript. K.H.K. and T.M.Q. provided X-rayed slices from the coral core retrieved 2004 outside La Parguera.

Author Information Reprints and permissions information is available at www.nature.com/reprints. The authors declare no competing financial interests. Correspondence and requests for materials should be addressed to J.N. (johan.nyberg@sgu.se).

METHODS

Vertical windshear. The correlation coefficient (r_S) between the observed number of major hurricanes and $|V_z|$ averaged over the whole MDR during August to October is –0.76 ($P < 0.001$; time interval 1949–2003; five-year moving average). Our proxies respond to surface (mainly easterly) winds that are related to this zonal overturning Walker circulation. r_S between the instrumental observed annual wind speed[30] shown (Fig. 3) and instrumental observed vertical windshear averaged over MDR in August-October from 1949 to 1992 is 0.90. r_S between the instrumental observed annual windspeed and the estimated V_z derived from the neural network algorithm from 1890 to 1990 is 0.85.

Coral records. Luminescence and reflectivity were measured in ~4-mm-thick slices, dried, whitened and cleaned of organic material and adherent contaminants[16,31], and cut parallel to the growth axis in massive *Montastraea faveolata* skeletons. The core outside Catalina Island, southeastern Dominican Republic was drilled in March 1999 and spans back to 1847, and the core outside Mona Island was drilled in May 1998 and spans back to 1684 (ref. 16). The two cores outside La Parguera, southwestern Puerto Rico, were drilled in February 1998 and 2004, respectively. Four U/Th dates retrieved at the University of Minnesota, together with density-band counting, demonstrate that the first core represents ages ranging from 1768 to 1957. The second core spans back to 1870 on the basis of density-band counting.

The luminescence and reflectivity of the coral slices were measured in a plate reader attached to a Perkin-Elmer Model LS 50B luminescence spectrometer. The plate scan speed was set to 30 mm min^{-1} and the excitation and emission slit widths to 2.5 mm. The measurements were made every 0.1 mm along the growth axis through a lamp with a diameter of 1 mm. An excitation wavelength of 390 nm and an emission wavelength of 490 nm were chosen[16,31]. The relative luminescence was calculated according to ref. 31, in which measurements of luminescence and reflectivity of coral slices are corrected using measurements of background and calcium carbonate standards. For the background standard a black plate with roughened surface was used on which the coral slices were laid down during measurements. The calcium carbonate standard used was Suprapur $CaCO_3$ 99.95 (Merck, Darmstadt, Germany).

Luminescence and reflectance were measured for both the background and calcium carbonate standards at the start and end of each luminescence and reflectance run. Beginning and end measurements were required to be within 2% of each other. Luminescence and reflectivity were measured at the same points along 3 to 6 different columellas (growth axis) through the coral cores avoiding visible gaps and holes. Similar results were obtained and the averaging results from the luminescence profiles were used.

Coral chronology. The luminescence profiles were converted to time series by setting annual luminescence minima to occur in summer. This is the approximate time when high-density bands precipitate in *Montastraea faveolata* in this region[32]. August, September and October for each year was then determined by measuring the extension rate and assuming a linear relationship between time and extension rate for the given year. The average relative luminescence in the August–October interval is used. Thus, this data refers to a seasonally specific relationship between trade winds (for example, $|V_z|$) and rainfall.

The youngest 30–40 mm of growth in the coral cores were omitted owing to the risk of contamination from the upper 6–8-mm-thick, anomalously high luminescence tissue layer, which is possibly associated with oxidized organics. Cross-dating characteristic luminescent bands between the different cores was applied[33]. After correcting ages the annual luminescence intensity values were standardized in each core. The maximum value was assigned to be 3 and the minimum value –3.

Multiproxy calibrations and reconstructions. Back propagation artificial neural networks were used for the reconstructions, because the nonlinear mapping of the input variables to the output variable inherent in artificial neural networks was found to provide better predictions than conventional linear regression analysis (see Supplementary Information). The correlation coefficients (r_S) between the reconstructed and instrumentally recorded $|V_z|$ and number of major hurricanes are 0.97 ($P < 0.001$, 1949–1990) and 0.92 ($P < 0.001$, 1944–1990), respectively, and the root-mean-square errors of predictions are 0.21 m s^{-1} for $|V_z|$ and 0.21 for hurricanes, respectively.

Warm-season (April–September) SSTs used in the hurricane activity and vertical wind shear reconstructions were retrieved from $5 \times 5^\circ$ grids[20]. The raw warm-season instrumental data, which were used to calibrate temperature reconstructions in ref. 20, were also used here in the training of the networks and in the reconstructions back to 1902. A comparison between the SST data used and the ERSST v2 data[22] averaged over a slightly larger region (10 to 26° N and 20 to 86° W) during August–October back to 1856 yields an r_S of 0.77 ($P < 0.001$). r_S between ERSST v2, averaged over the region referred to above, and the instrumental $|V_z|$, averaged over the MDR, is –0.38 ($P < 0.01$; 1950–2003). r_S between ERSST v2 and number of *G. bulloides* is –0.43 ($P < 0.001$; 1900–1990). r_S between ERSST v2 and the master luminescence record is 0.28 ($P < 0.05$; 1950–2000).

No significant statistical relationships are found between the AMO index of ref. 26 and the major hurricane and $|V_z|$ records (1730–1985). The r_S between the AMO index of ref. 6 and the major hurricane record is 0.32 ($P < 0.001$; 1858–2003) and that between the AMO index of ref. 6 and $|V_z|$ is -0.22 ($P < 0.01$; 1858–2003). The r_S between TSI and the major hurricane record is –0.37 ($P < 0.001$; 1730–2003) and that between TSI and $|V_z|$ is 0.44 ($P < 0.001$; 1730–2003) using the instrumental major hurricane observations since 1944 and $|V_z|$ since 1949 (Fig. 4). Observational bias adjustments are taken into account by using 52 m s^{-1} as a threshold for major hurricanes during the time period 1944–1969.

31. Barnes, D. J., Taylor, R. B. & Lough, J. M. Measurement of luminescence in coral skeletons. *J. Exp. Mar. Biol. Ecol.* **295**, 91–106 (2003).
32. Watanabe, T. A., Winter, A., Oba, T., Anzai, R. & Ishioroshi, H. Evaluation of the fidelity of isotope records as an environmental proxy in the coral *Montastraea*. *Coral Reefs* **21**, 169–178 (2002).
33. Hendy, E. J., Gagan, M. K. & Lough, J. M. Chronological control of coral records using luminescent lines and evidence for non-stationary ENSO teleconnections in northeast Australia. *Holocene* **13**, 187–199 (2003).